Communications on Applied Nonlinear Analysis
ISSN: 1074-133X
Vol 32 No. 9s (2025)

Improving Distribution System Performance using the Optimal Placement of DGs and Reconfiguration for Different Load Models

Ravi Kant Yadav[1] , Dibya Bharti[2] , Mala De[3]

[1] (PhD Scholar), Department of Electrical Engineering, National Institute of Technology, Patna, India, raviy.phd19.ee@nitp.ac.in

[2]Assistant professor, Department of electrical engineering, Bhagalpur college of engineering, Bhagalpur, Bihar 813210, dibya_minu1@rediffmail.com

[3]Associate professor, Department of Electrical Engineering, National Institute of Technology, Patna, India, mala@nitp.ac.in

Article History:

Received: 12-11-2024

Revised: 10-12-2024

Accepted: 15-01-2025

Abstract: The distribution system often gets significant power losses due to voltage drops. To address this issue, various techniques have been proposed in the literature, predominantly focusing on single-load models. This study introduces a methodology aimed to minimizing system losses and enhancing voltage profiles by integrating distributed generation (DG) placement with network reconfiguration (NR) for different load models. The analysis considers constant power (CP), constant current (CI), constant impedance (CZ), and constant impedance, current and power (ZIP) load models under varying load conditions. The methodology employs the index vector approach and a modified whale optimization algorithm to identify the optimal placement of DGs. A load escalation rate of 7% is factored in for planning the distribution system over a five-year. The approach is validated using modified 33-bus and 69-bus radial distribution systems (RDS), with performance com- pared against genetic algorithm (GA) and particle swarm optimization (PSO) techniques for the Constant power load model. The results indicate that combining system reconfiguration with DG placement effectively reduces system losses while enhancing voltage stability.

Keywords: Radial distribution system (RDS), Modified whale optimization algorithm (MWOA), Constant power load model (CPLM), Constant current load model (CCLM), Constant impedance load model (CILM), and Constant impedance, current and power load model (ZIPLM).

1 Introduction

Managing and controlling of distribution networks becomes more complex with fluctuating load demand, particularly in areas with high load density. Fixed network topologies, combined with varying load demands, often lead to significant power losses in RDS, posing challenges for operators. Techniques such as optimal distributed generation placement (ODGP) and network reconfiguration (NR) are widely utilized to address these issues.

NR involves modifying the configuration of feeders by adjusting the operational states of sectionalizing and tie switches. DGs are small-scale power generation units, varying from a few kW to MW, directly integrated into the current distribution networks. This reconfiguration approach is nonlinear in nature and helps alleviate overloaded feeders, thereby reducing system losses.

Researchers have explored the use of DGs with different load models, as well as employing series voltage regulators and shunt capacitors, to maintain voltage levels and minimize losses in distribution systems. However, shunt capacitors and series voltage regulators have limitations. Shunt capacitors cannot provide continuously adjustable reactive power, and series voltage regulators operate slowly due to their stepwise adjustments.

Strategically placing DGs with different load models in distribution systems (DS) offers an effective solution for improving system performance and addressing the limitations of constant load models, shunt capacitors, and series voltage regulators.

1.1 Concepts and motivations

Renewable energy has been growing rapidly due to increasing concern for environmental sustainability and the wide adaption of EVs in transport sector. As a result, the integration of DGs and EV charging stations has become a critical area of research in the field of power systems. The optimal placement of DGs and reconfiguration can significantly improve the performance of the distribution system. This study aims to address these challenges by proposing a comprehensive framework for the optimal integration of DG placement and reconfiguration of DS. In this study, propose the minimization of distribution system power losses, improvement of the voltage profile. The different load models taking into the optimization model, the placement of DG and reconfiguration can be effectively optimized to enhance the overall performance of the distribution system. Moreover, the proposed framework considers the dynamic nature of load, ensuring that the optimal placement and allocation are robust under varying load conditions. Additionally, the varying load profiles are accounted for to ensure that the distribution system can accommodate different demand scenarios, leading to improved reliability and efficiency [6].

1.2 Existing Work:

Various strategies have been proposed in the literature to address the problem of distribution system reconfiguration (DSR) for minimizing power losses. One heuristic method focuses on network reconfiguration to achieve loss reduction [1]. Recent advancements include the chaotic stochastic fractal search algorithm (CSFSA), which integrates chaotic behavior into the traditional stochastic fractal search algorithm (SFSA) to enhance distribution system reconfiguration performance [2]. Several approaches have also been introduced for solving the DG allocation problem. For instance, one method utilizes the whale optimization algorithm to optimize DG placement and sizing, aiming to reduce losses, improve voltage profiles, and enhance reliability while considering residential, commercial, and industrial loads [3]. Another study presents a strategy for placing D-STATCOMs with and without NR for various load models, including CPLM, CILM, CZLM, and ZIPLM, under load variation conditions [4]. The salp swarm algorithm has been applied to concurrently address NR and DG allocation, demonstrating effectiveness in minimizing power loss and voltage deviation under different scenarios, such as isolated DG placement, isolated NR, and NR post-DG placement [5]. Another innovative approach leverages the artificial ecosystem optimizer to integrate DG and capacitor allocation for recon- figuring power distribution systems, with practical application demonstrated on Egypt's 59-bus Cairo distribution system [6]. Additionally, efficient techniques have been developed to simultaneously optimize system reconfiguration and DG placement. These methods aim to minimize power loss, improve voltage profiles, balance loads and feeders, and minimize switching

operations. For example, an improved moth swarm algorithm has been employed for test systems with 33 and 84 nodes, achieving multiple objectives effectively [7,8,9]. In [10], the authors discussed distribution NR and DG placement for minimizing power losses and optimizing voltage in DS via the WOA and evaluated its effectiveness on 33-bus and 69-bus grids. A multi objective approach for NR and DG allocation in DS, aiming to minimize losses and operational costs while maximizing stability, was presented in [11]. When the TFN is used to model load uncertainty, the multi objective hybrid big bang–big crunch (MOHBB-BC) method generates diverse Pareto solutions, considering realistic scenarios despite greater losses. The authors of [12] addressed optimal DG allocation, used a hybrid gray wolf optimizer that was applied to various DSs, markedly reduced losses, enhanced voltage profiles without algorithm tuning, outperformed other methods and identified global optimal solutions. Multi objective strategy that integrates NR with DG allocation, and uses evolutionary techniques based on Pareto optimality and fuzzy set theory to achieve optimal configurations across multiple criteria was introduced in [13]. Paper [14] proposed a simultaneous approach and combined NR and capacitor placement in radial distribution networks, employing Johnson's algorithm and an adaptive whale optimization algorithm, which is more efficient than the previous methods in the literature. In [15,16], the authors discussed a genetic algorithm to optimize DG integration, considering electric vehicles (EVs) to reduce power losses and enhance voltage profiles to increase electrical power demand on standard 33- and 69-bus systems under various scenarios. the authors explore the advantages of modern DG technologies compared to traditional power systems, focusing on economic, environmental, and technical aspects. Additionally, it examines various DG technologies that can be integrated into power distribution net- works to achieve enhanced loss reduction [17,18]. The impact of DG penetration levels on active and reactive power losses, voltage profiles, and node voltage deviations across various load types will be analyzed [19,20]. A comprehensive discussion on energy and power losses is included [21,22]. The DG units help manage PEV charging impacts on distribution systems, along with addressing uncertainties in renewable energy, PEV behavior, and time-varying loads, while analyzing reliability through power interruption metrics [23]. Most studies have primarily focused on either distributed generation (DG) allocation or NR to improve the performance of distribution systems (DS). Only a limited number of researchers have explored the simultaneous implementation of NR and DG allocation in distribution networks. A review of the literature reveals that many studies model systems using single load models, despite the fact that real-world power systems exhibit varying load characteristics. In practical scenarios, loads can be represented as CPLM, CILM, CZLM, ZIPLM with load variations. To address these challenges, this study proposes a methodology that integrates optimal placement of DGs and reconfiguration in radial distribution systems (RDS) while considering different load models.

1.3 Novelties of Paper

This paper proposes a novel methodology for optimal placement of DGs and reconfiguration, addressing CPLM, CILM, CZLM, and ZIPLM under varying load. This studies have focused on the synergies among renewable energy generation, reconfiguration, and distribution system operation. This research can maximize the utilization of DG resources, minimize grid congestion, and promote the efficient integration of electric vehicles into the transportation and energy sectors. This integrated approach contributes to overall system resilience, sustainability, and cost-effectiveness.

Novel optimization techniques have emerged to address multiple conflicting objectives

simultaneously. These objectives may include minimizing real power losses, improving the voltage profile, reducing greenhouse gas emissions, and enhancing grid reliability.

1.4 This Paper's Contributions

This paper proposes a methodology to minimize system losses and enhance voltage profiles by integrating DG placement with subsequent NR for various load models. The approach focuses on reducing active and reactive power losses through reconfiguration after optimally placing DGs in RDS to improve voltage profiles. The effectiveness of the proposed method is demonstrated using modified 33- bus and 69-bus RDSs with high DG penetration, considering different load models. Numerical results validate the improvements in voltage deviation and the reduction of total power losses achieved by this approach. The proposed methodology is compared against existing techniques, such as the GA and particle PSO, for different load model scenarios, including modified 33-bus RDSs.

1.5 Organization of paper

This paper is structured as, Section 2 outlines the formulation of the problem statement for presented approach and methodology, focusing on minimizing voltage deviation and minimizing system losses. In Section 3, To evaluate the performance of the formulated approach, it is applied to a modified 33-bus RDS and a modified 69-bus RDS under various operational scenarios, incorporating multiple DGs. Section 4 presents the results and their analysis for these systems. Section 5 provides a comparative evaluation of the proposed approach with existing methods, including particle PSO and the GA, specifically for the CP load model on the modified 33-bus RDS. Finally, Section 6 concludes the paper by summarizing the key findings.

2 Problem Formulation

The proposed methodology aims to minimize active power losses in the DS by combining optimal DG placement with NR, considering CPLM, CILM, CZLM, and ZIPLMs. The index vector method is utilized to identify the optimal DG location, while the modified whale optimization algorithm (MWOA) is applied to determine the optimal DG size. Additionally, the MWOA is employed for NR to further enhance system performance.

In distribution systems, lower voltage levels lead to greater power losses compared to transmission systems, primarily due to higher current flows and the comparatively higher resistance of distribution lines, and this is computed as $Ploss = \sum_i^n I_i^2 R_i$ The aim of this paper is to minimize active power loss. Therefore, the objective function for the proposed methodology is as follows:

$$F = (Pl) = Min \sum_i^n I_i^2 R_i \quad (1)$$

This paper aims to reduce active power losses, where the current is denoted by I_i, R_i represents the resistance, and n signifies the number of buses in power the system. The constraints are

$$\text{Bus Voltage: } 0.95 \leq V_i \leq 1.05$$

$$\text{Power balance: } P_g + \sum_{k=1}^{N} P_{dg} = P_d + P_{loss}$$

Maximum and minimum limits of DG: $50 \leq P_{dg} \leq 2500$

DG type I is assigned to the kW limit, DG type II to the kVAR limit, and DG type III to the kVA limit.

2.2. Electrical Load Modeling: In the case of static load models, the real and reactive power can be expressed using an exponential relationship as follows:

$$P = P_0(\frac{V}{V_0})^{K_p} \quad (2)$$

$$Q = Q_0(\frac{V}{V_0})^{K_q} \quad (3)$$

At the nominal voltage V_0 of the bus, the active power is denoted as P_0 and the reactive power as Q_0. The bus load voltage is V, and the load exponents are $K_p$and K_q [4]. For the CPLM, K_p= K_q=0. For the CILM,K_p= K_q=1. For the CZLM, K_p= K_q=2.

$$P = P_0[\alpha_p(\frac{V}{V_0})^2] + \beta_p(\frac{V}{V_0}) + \gamma_p] \quad (4)$$

$$Q = Q_0[\alpha_q(\frac{V}{V_0})^2] + \beta_q(\frac{V}{V_0}) + \gamma_q] \quad (5)$$

Where $\alpha_p, \beta_p, \gamma_p, \alpha_q, \beta_q \; and \; \gamma_q$are ZIPLM coefficients. The sum of the coefficients for the ZIPLM for both active (P) and reactive (Q) power are normalized to 1. α_p+ β_p+ γ_p = 1, α_q + β_q+ γ_q= 1. For the suggested methodology, α_p= α_q= 0.1, β_p= β_q= 0.1, γ_p= γ_q= 0.8. P_0 represents the real power consumed at a reference voltage V_0 and Q_0 represents reactive power consumed at the reference voltage.

2.2.1 Load variation model. - $Load_t = Load_0 \times (1 + y)$ (6)

In the 33-bus test system, y represents the annual growth rate, and t denotes the time period during which the feeder supports the load, and y = 0.07 and t = 5 year.

2.2.2 Vector Indexing Technique [4] - The vector-based indexing technique [3] can be utilized to identify the best DG placements. For bus *n*, the corresponding index vector is defined as

$$Index[n] = \frac{1}{V^2[n]} + \frac{I_q^{(K)}}{I_p^{(k)}} \frac{Q_{eff[n]}}{Q_{Total(n)}} \quad (7)$$

In the k[th] branch, $I_q^{(K)}$ corresponds to the real part of the current, while $I_p^{(k)}$ represents the imaginary part. The reactive load and voltage at the n^{th} bus are denoted as $Q_{eff[n]}$ and $V_{[n]}$ respectively, whereas $Q_{Total(n)}$ signifies the overall reactive load at that bus.

2.3. MWOA

The proposed method uses the modified whale optimization algorithm, which is derived from WOA, a new metaheuristic method inspired by the cooperative behavior of humpback whales. When tested on 29 math problems and 6 structural design challenges, the WOA shows strong performance compared with other modern algorithms and conventional approaches [16]. The mathematical framework of the WOA encompasses processes such as encircling the prey, employing the bubble-net

hunting strategy, and searching for prey. These steps are detailed below:

2.3.1. Encapsulating prey - In WOA, the target prey denotes the best available solution. Other agents strive to enhance their positions to achieve the status of the best search agent. The behavioral model is illustrated below:

$$\vec{X}(t+1) = \vec{X}*(t) - \vec{U}.\vec{Z} \quad (8)$$

$$\vec{Z} = [W.X*t - X.t] \quad (9)$$

$$\vec{U} = 2.\vec{a}.\vec{r} - \vec{a} \quad (10)$$

$$\vec{W} = 2.\vec{r} \quad (11)$$

Where $\vec{X}*$ represents the best solution, X denotes the position vector, Z is a random variable influencing the update, t indicates the current iteration, $\vec{U}$and $\vec{W}$ are coefficient vectors, $\vec{a}$ is a diminishing factor with values ranging from 2 to 0, and $\vec{r}$ is a randomly selected vector within the range [0, 1]

2.3.2. Bubble net foraging method – This paper presents two methods for hunting.

a. Contracting encircling of the prey: Here, a is a vector within the range [-a, a], with the value of 'a' decreasing from 2 to 0. In this case, the position U is randomly initialized within the interval [-1, 1]. The new position of 'a', which is bounded by $0 \leq a \leq 1$, is determined between the initial location and the current optimal agent's position in a 2D space, as shown in Equation 8, moving from (X, Y) to (X^*,Y^*)

b. Spiral movement updating - The spiral equation is employed to model the helical movement.

$$\vec{X}(t+1) = \vec{Z}.e^{bl}.\cos(2\pi l) + \vec{X}* \quad (12)$$

Were as e^{bl} suggests an exponential component, where b and l are parameters and $\cos(2\pi l)$introduces an oscillatory (periodic) influence. During hunting, whales approaching their prey from two separate directions simultaneously. For the next two methods used to update the positions of the whales, having a 50% probability is applied to determine which approach will be used.

$$\vec{X}(t+1) = \begin{cases} \vec{X}*(t) - \vec{U}.\vec{Z} & \text{if } p < 0.5 \\ \vec{Z'}.e^{bl}.\cos(2\pi l) + \vec{X}* & \text{if } p \geq 0.5 \end{cases} \quad (13)$$

c. Search for prey - Instead of using the most efficient search agent, the global optimal values are revised through a randomly selected search agent.

$$\vec{Z} = [\vec{W}.\vec{X}\vec{r}\vec{a}\vec{n}\vec{d} - \vec{X}] \quad (14)$$

$$X(t+1) = \vec{X}\vec{r}\vec{a}\vec{n}\vec{d} - \vec{U}\vec{Z} \quad (15)$$

$\vec{X}\vec{r}\vec{a}\vec{n}\vec{d}$is the current iteration's random value.

2.4. DG Placement Optimization: An optimization algorithm is required to determine the optimal locations and capacities of DGs in the DS and TPL and TQL represents total active power and total reactive power.

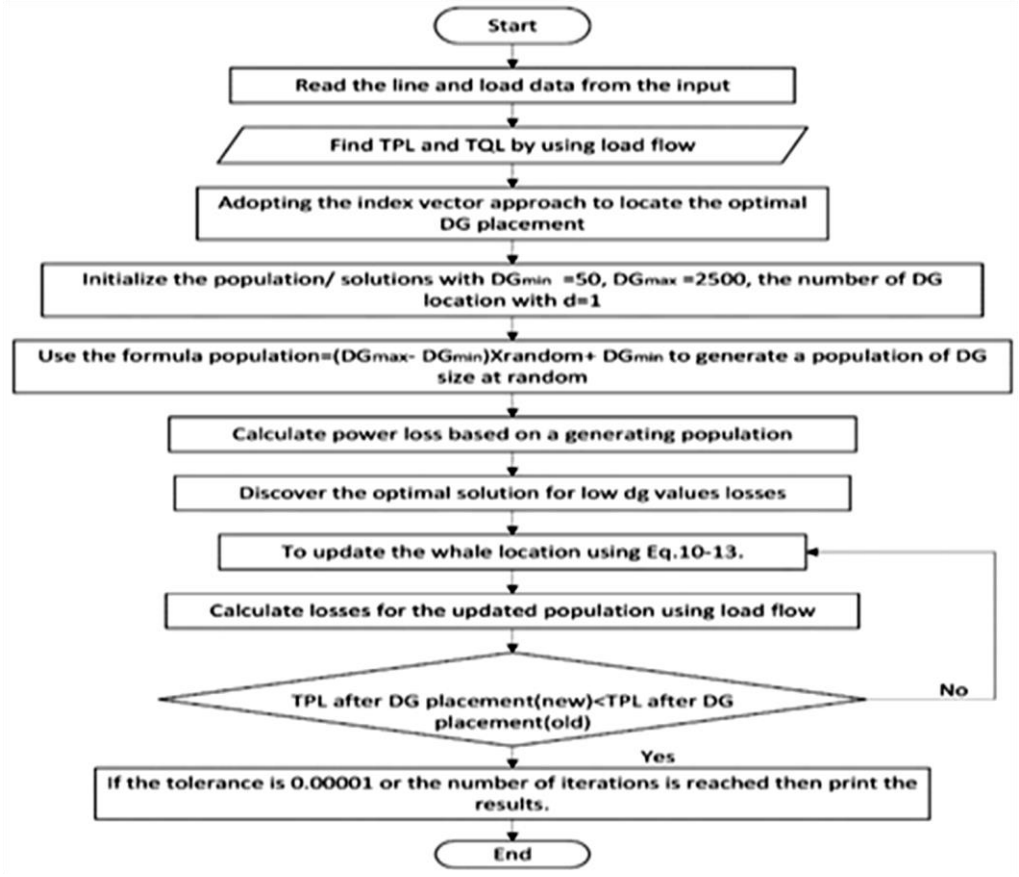

Fig.1. Flow chart of proposed DGs placement.

2.5. Distribution system reconfiguration: MWOA is utilized for NR to reduce system losses and improve the voltage profile. A flowchart depicting the proposed methodology is shown in Fig. 2.

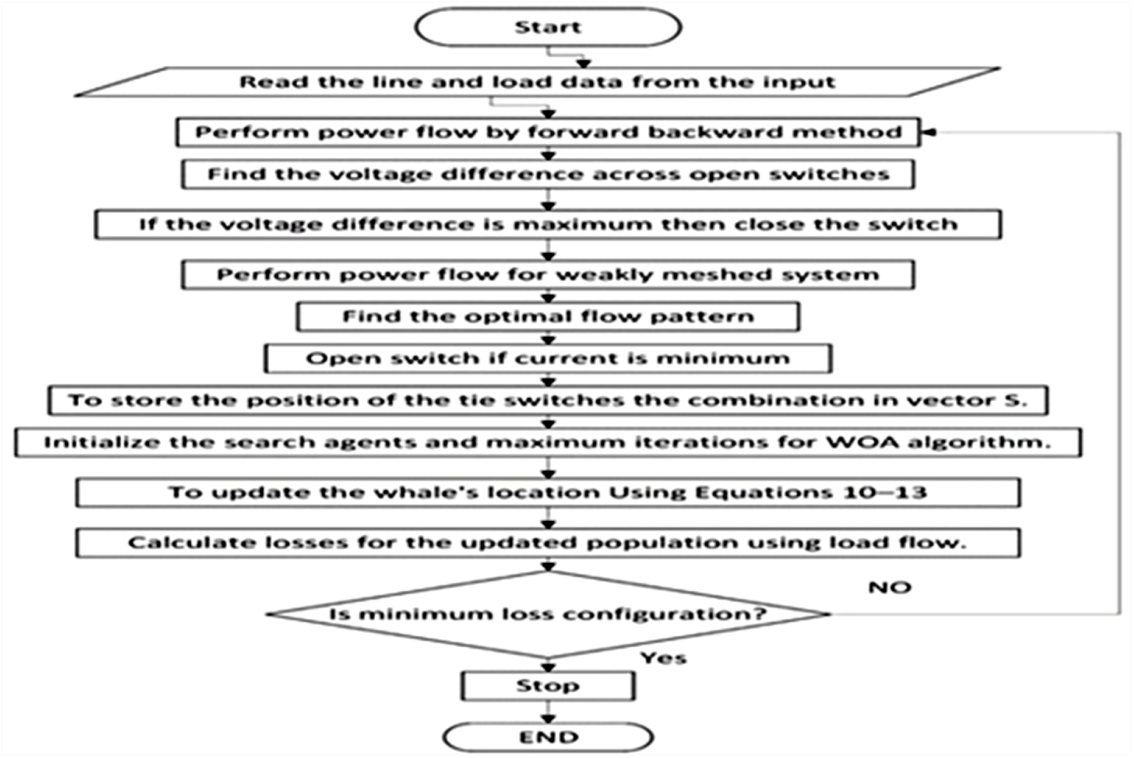

Fig.2. Algorithm Flow for Reconfiguration.

3 Implementation of the proposed technique

To apply the proposed method, two modified radial distribution systems are considered: 33-bus and a 69-bus, both integrated with multiple DGs units. In the 33-bus system, three solar generation units of 10 kW, 20 kW, and 35 kW are added at buses 6, 21, and 26, respectively, as illustrated in Fig. 3a. Similarly, in the 69-bus system, six solar generation units with capacities of 25.0 kW, 30.0 kW, 20.0 kW, 35.0 kW, 40.0 kW, and 45.0 kW are connected at buses 33, 69, 62, 65, 44, and 46, as shown in Fig. 3b.

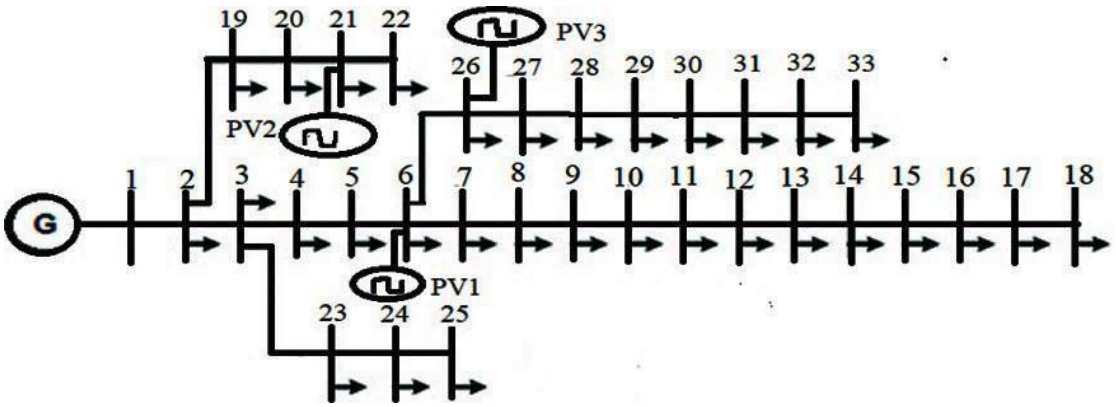

Fig. 3a. Modified 33-bus RDS

Table.1. Load Data and Line Data of modified 33 bus test system

Load data specifies the active (P) and reactive (Q) power at each bus and Line data specifies the connection between buses and the impedance (R, X).

S. No.	From Bus	To Bus	**Load (P)** (kW)	**Load (Q)** (kVAR)	R (p.u.)	X (p.u.)
1	1	2	100	60	0.0922	0.0470
2	2	3	90	40	0.4930	0.2511
3	3	4	120	80	0.3660	0.1864
4	4	5	60	30	0.3811	0.1941
5	5	6	60	20	0.8190	0.7070
6	6	7	200	100	0.1872	0.6188
7	7	8	200	100	0.7114	0.2351
8	8	9	60	20	1.0300	0.7400
9	9	10	60	20	1.0440	0.7400
10	10	11	45	30	0.1966	0.0650
11	11	12	60	35	0.3744	0.1238
12	12	13	60	35	1.4680	1.1550
13	13	14	120	80	0.5416	0.7129
14	14	15	60	10	0.5910	0.5260
15	15	16	60	20	0.7463	0.5450
16	16	17	60	20	1.2890	1.7210
17	17	18	90	40	0.7320	0.5740

18	18	19	90	40	0.1640	0.1565
19	19	20	90	40	1.5042	1.3554
20	20	21	90	40	0.4095	0.4784
21	21	22	90	40	0.7089	0.9373
22	22	23	90	50	0.4512	0.3083
23	23	24	420	200	0.8980	0.7091
24	24	25	420	200	0.8960	0.7011
25	25	26	60	25	0.2030	0.1034
26	26	27	60	25	0.2842	0.1447
27	27	28	60	25	1.0590	0.9337
28	28	29	120	70	0.8042	0.7006
29	29	30	200	600	0.5075	0.2585
30	30	31	150	70	0.9744	0.9630
31	31	32	210	100	0.3105	0.3619
32	32	33	60	40	0.3410	0.5302
33	8	21	0	0	2.0000	2.0000
34	9	15	0	0	2.0000	2.0000
35	12	22	0	0	2.0000	2.0000
36	18	33	0	0	0.5000	0.5000
37	25	29	0	0	0.5000	0.5000

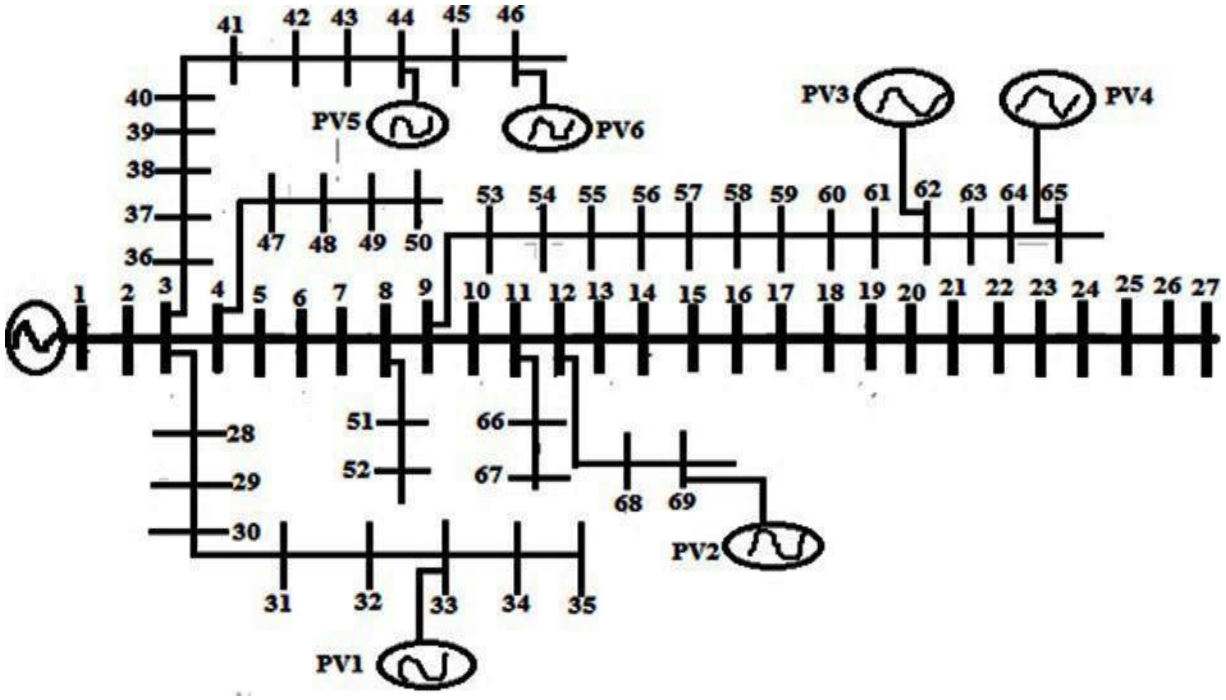

Fig. 3b. Modified 69-bus RDS

In the analyzed system, centralized power generation system is located at bus 1. The total power demand is 3650 kW for the modified 33-bus system and 3771 kW for the modified 69-bus system.

Table.2. Load Data and Line Data of modified 69 bus test system

Load data specifies the active (P) and reactive (Q) power at each bus and Line data specifies the connection between buses and the impedance (R, X).

S. No.	From Bus	To Bus	**Load (P)** (kW)	**Load (Q)** (kVAR)	R (p.u.)	X (p.u.)
1	1	2	0	0	0.0005	0.0012
2	2	3	0	0	0.0005	0.0012
3	3	4	0	0	0.0015	0.0036
4	4	5	0	0	0.0251	0.0294
5	5	6	2.6	2.2	0.366	0.1864
6	6	7	40.4	30	0.3811	0.1941
7	7	8	75	54	0.0922	0.047
8	8	9	30	22	0.0493	0.0251
9	9	10	28	19	0.819	0.2707
10	10	11	145	104	0.1872	0.0619
11	11	12	145	104	0.7114	0.2351
12	12	13	8	5	1.03	0.34
13	13	14	8	5.5	1.044	0.345
14	14	15	8	5.5	1.058	0.3496
15	15	16	45.5	30	0.1966	0.065
16	16	17	60	35	0.3744	0.1238
17	17	18	60	35	0.0047	0.0016
18	18	19	0	0	0.3276	0.1083
19	19	20	1	0.6	0.2106	0.069
20	20	21	114	81	0.3416	0.1129
21	21	22	5	3.5	0.014	0.0046
22	22	23	0	0	0.1591	0.0526
23	23	24	28	20	0.3463	0.1145
24	24	25	0	0	0.7488	0.2475
25	25	26	14	10	0.3089	0.1021
26	26	27	14	10	0.1732	0.0572
27	27	28	26	18.6	0.0044	0.0108
28	28	29	26	18.6	0.064	0.1565
29	29	30	0	0	0.3978	0.1315
30	30	31	0	0	0.0702	0.0232
31	31	32	0	0	0.351	0.116
32	32	33	14	10	0.839	0.2816
33	33	34	19.5	14	1.708	0.5646
34	34	35	6	4	1.474	0.4873
35	35	36	26	18.55	0.0044	0.0108

36	36	37	26	18.55	0.064	0.1565
37	37	38	0	0	0.1053	0.123
38	38	39	24	17	0.0304	0.0355
39	39	40	24	17	0.0018	0.0021
40	40	41	1.2	1	0.7283	0.8509
41	41	42	0	0	0.31	0.3623
42	42	43	6	4.3	0.041	0.0478
43	43	44	0	0	0.0092	0.0116
44	44	45	39.22	26.3	0.1089	0.1373
45	45	46	39.22	26.3	0.0009	0.0012
46	46	47	0	0	0.0034	0.0084
47	47	48	79	56.4	0.0851	0.2083
48	48	49	384.7	274.5	0.2898	0.7091
49	49	50	384.7	274.5	0.0822	0.2011
50	50	51	40.5	28.3	0.0928	0.0473
51	51	52	3.6	2.7	0.3319	0.1114
52	52	53	4.35	3.5	0.174	0.0886
53	53	54	26.4	19	0.203	0.1034
54	54	55	24	17.2	0.2842	0.1447
55	55	56	0	0	0.2813	0.1433
56	56	57	0	0	1.59	0.5337
57	57	58	0	0	0.7837	0.263
58	58	59	100	72	0.3042	0.1006
59	59	60	0	0	0.3861	0.1172
60	60	61	1244	888	0.5075	0.2585
61	61	62	32	23	0.0974	0.0496
62	62	63	0	0	0.145	0.0738
63	63	64	227	162	0.7105	0.3619
64	64	65	59	42	1.041	0.5302
65	65	66	18	13	0.2012	0.0611
66	66	67	18	13	0.0047	0.0014
67	67	68	28	20	0.7394	0.2444
68	68	69	28	20	0.0047	0.0016
69	11	43	0	0	0.5	0.5
70	13	20	0	0	0.5	0.5

4 Results and Discussion

The analysis was performed using MATLAB version 9.0 on a Windows 10 system (Intel® Core™ i3 Processor, 3.30 GHz, 4 GB RAM). The results were obtained for DG placement, both with and without network reconfiguration, in the modified 33-bus and 69-bus RDS under various load models (CPLM, CILM, CZLM, and ZIPLM). The system's performance, including voltage profiles, power loss, and other metrics, was evaluated across different load models. The following three scenarios were considered for the analysis:

- **Case 1**: Only NR of the RDS.
- **Case 2**: Only DGs placement of the RDS.
- **Case 3**: NR after placement of DGs in the RDS.

4.1 CPLM Analysis for the Modified 33-bus RDS

The CPLM for both cases is provided in Table 3. The analysis shows a significant reduction in line loss, which decreases from 198.7791 kW to 23.4077 kW in Case 2. In Case 3, the line loss is further reduced to 19.6848 kW. This reduction in active power loss is achieved by installing a total of six DGs units at the following bus locations and capacities: bus 25 (372 kW), bus 28 (459 kW), bus 32 (500 kW), bus 33 (500 kW), bus 11 (391 kW), and bus 17 (500 kW). Fig. 4 illustrates the improvement in voltage profile in Case 3 compared to Case 2. It also highlights, a slightly higher voltage deviation is observed between buses 17 and 18.

Table 3. Results analysis for case2 and case3 for CPLM (modified 33-bus system)

PARAMETERS	BASE_CASE	Case2	Case3
Total Real Power Loss(TPL)	198.7913	23.4017	19.6848
Total Reactive Power Loss(TQL)	132.682	19.0626	16.3742
Tie Switch Number	33 34 35 36 37	33 34 35 36 37	17 11 35 33 25
DG Location	NIL	25 28 32 33 11 17	NIL
DG Size (P kW)	NIL	372 459 500 500 391 500	NIL
DG Size Q (kVAR)	NIL	180.1678 222.3038 242.1611242.1611 189.3699 242.1611	NIL
Total DG size (kW)	NIL	2722	NIL
Voltage Minimum	0.91377	0.99027	0.99283

Table 4. Results Analysis for case2 and case3 for CILM (modified 33-bus system)

PARAMETERS	BASE_CASE	Case2	Case3
TPL	171.6116	31.5958	28.1628
TQL	114.2673	20.6153	19.881
Tie Switch Number	33 34 35 36 37	33 34 35 36 37	27 33 10 14 15
DG Location	NIL	17 21 25 29 31 8	NIL
DG Size P (kW)	NIL	253 176 465 436 292 328	NIL
DG Size Q (kVAR)	NIL	122.5335 85.24069 225.2098 211.1644 141.4221 158.8577	NIL
Total DG(kW)	NIL	1950	NIL
Voltage Minimum	0.92044	0.9695	0.9780

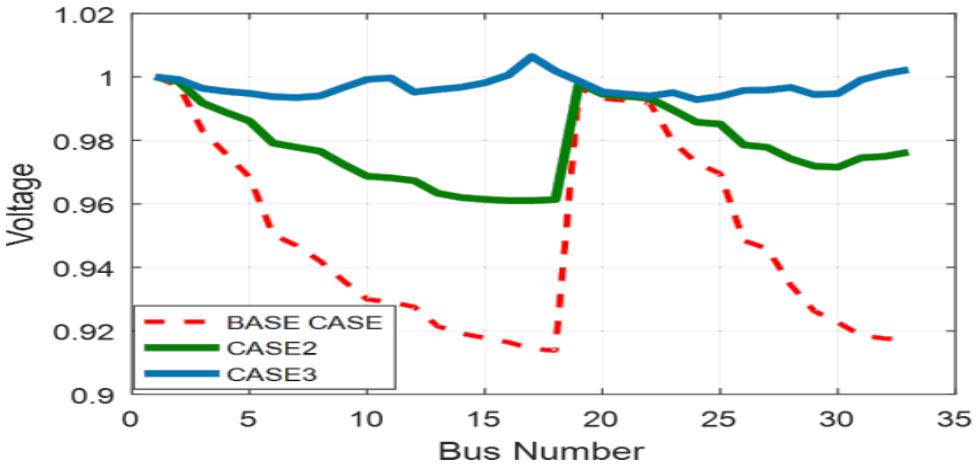

Fig. 4. Voltage variation for the CPLM

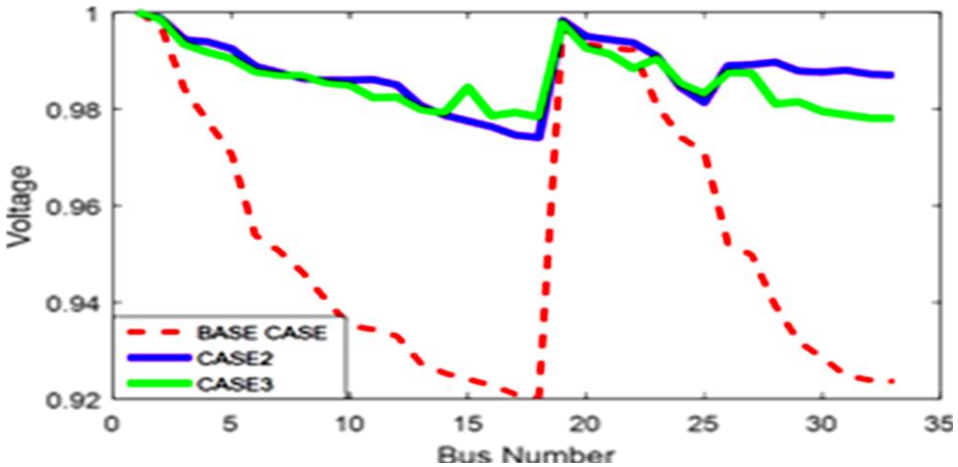

Fig. 5. Voltage variation for the CILM

4.2 CILM Analysis for the Modified 33-bus RDS

Table 4 presents the results for the CILM, comparing both cases. The analysis reveals a reduction in line loss from 171.6116 kW to 31.5958 kW in Case 2, and further to 28.1628 kW in Case 3. This reduction in active power loss is achieved by placing six DGs units at the following bus locations and capacities: bus 17 (253 kW), bus 21 (176 kW), bus 25 (465 kW), bus 29 (436 kW), bus 31 (292 kW), and bus 8 (328 kW). Fig. 5 illustrates that the voltage deviation in Case 3 closely follows the trend observed in Case 2.

Table 5. Results analysis for case2 and case3 for CZLM (modified 33-bus system)

PARAMETERS	BASE_CASE	Case2	Case3
TPL	151.8268	22.3601	29.2304
TQL	100.8949	16.5125	22.2232
Tie Switch Number	33 34 35 36 37	33 34 35 36 37	36 12 7 26 11
DG Location	NIL	15 27 29 33 3 8	NIL
DG Size P (kW)	NIL	340 328 287 500 500 260	NIL
DG Size Q (kVAR)	NIL	164.6695 158.8577 139.0004 242.1611 242.1611 125.9237	NIL
Total DG(kW)	NIL	2215	NIL
Voltage Minimum	0.92562	0.98258	0.9772

Table 6. Results analysis for case2 and case3 for ZIPLM (modified 33-bus system)

PARAMETERS	BASE_CASE	Case2	Case3
TPL	191.627	30.817	26.637
TQL	127.828	22.1290	20.4750
Tie Switch Number	33 34 35 36 37	33 34 35 36 3	8 28 34 7 14
DG Location	NIL	5 14 16 29 33 3	NIL
DG Size P (kW)	NIL	270 422 365 500 445 183	NIL
DG Size Q (kVAR)	NIL	130.767 204.384 176.778 242.161 215.523 88.6309	NIL
Total DG(kW)	NIL	2185	NIL
Voltage Minimum	0.9155	0.981	0.981

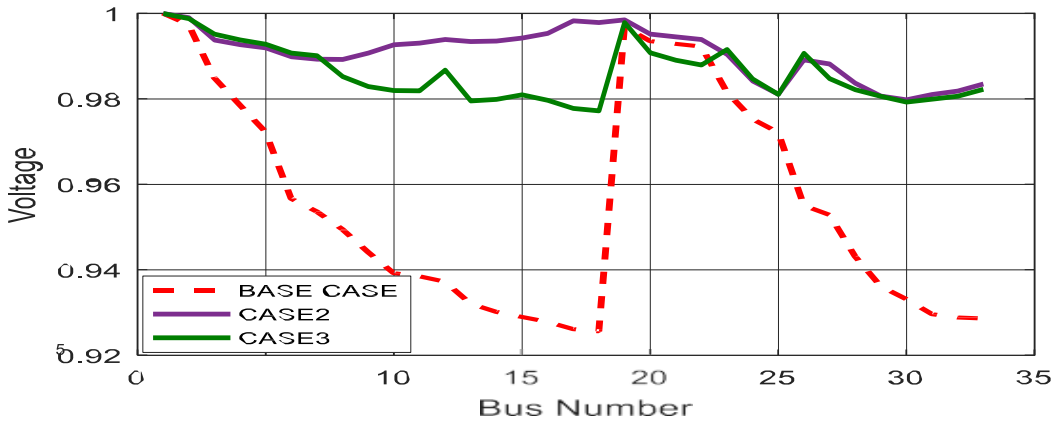

Fig. 6. Voltage profile for CZLM

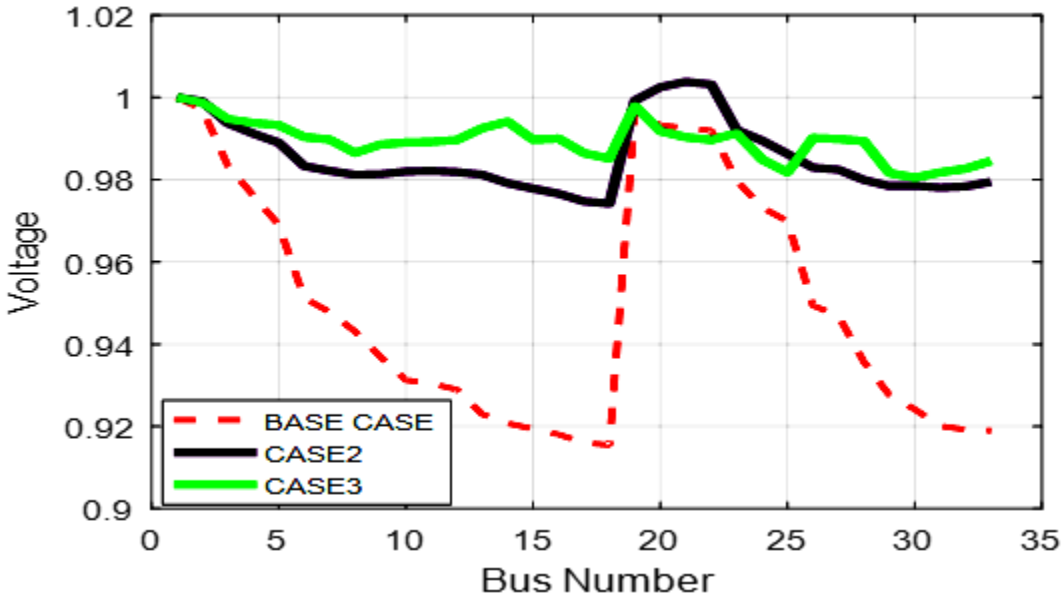

Fig. 7. Voltage profile for ZIPLM

4.3 CZLM Analysis for the Modified 33-bus RDS

Table 5 compares the results for the CZLM in both cases. The findings show that line loss decreases from 151.8268 kW to 22.3601 kW in Case 2, and further to 29.2304 kW in Case 3. This reduction in real power loss is achieved by installing six DGs units at the following bus locations and capacities: bus 15 (340 kW), bus 27 (328 kW), bus 29 (287 kW), bus 33 (500 kW), bus 3 (500 kW), and bus 8 (260 kW). Fig. 6 demonstrates that the voltage deviation in Case 3 is lower than in Case 2, indicating that reconfiguration is unnecessary after DG placement.

4.4 ZIPLM Analysis for the Modified 33-bus RDS

Table 6 presents the results for the ZIPLM in both cases. The analysis reveals that line loss decreases from 191.6269 kW to 30.817 kW in Case 2, and further reduces to 26.6369 kW in Case 3. This reduction in real power loss is achieved by installing six DGs units at the following bus locations and capacities: bus 5 (270 kW), bus 14 (422 kW), bus 16 (365 kW), bus 29 (500 kW), bus 33 (445 kW), and bus 3 (183 kW). Fig. 7 illustrates that the voltage deviation in Case 3 is improved compared to Case 2. The voltage deviation in Case 3 is improved compared to Case 2, with execution times of 2285.256 seconds for Case 3 and 3.2195 seconds for Case 2.

4.5 CPLM Analysis for the Modified 69-bus RDS

Table 7 presents the results for the CPLM in both cases. The analysis shows that line loss decreases from 214.2445 kW to 22.2445 kW in Case 2, and further reduces to 15.427 kW in Case 3. This reduction in real power loss is achieved by installing six DGs units at the following bus locations and capacities: bus 2 (500 kW), bus 63 (500 kW), bus 68 (500 kW), bus 59 (500 kW), bus 61 (500 kW), and bus 11 (500 kW). Fig. 8 illustrates that the voltage profile is significantly lower between buses 11 and 28, and between buses 50 and 64. The voltage deviation in Case 3 is improved compared to Case 2, with execution times of 2285.256 seconds for Case 3 and 3.2195 seconds for Case 2.

Table 7. Results analysis for case2 and case3 for CPLM (modified 69-bus system)

PARAMETERS	BASE_CASE	Case2	Case3
TPL	214.244	20.952	15.427
TQL	97.442	13.311	17.1647
Tie Switch Number	69 70 71 72 73	69 70 71 72 73	14 5 19 54 64
DG Location	NIL	2 63 68 59 61 11	NIL
DG Size P (kW)	NIL	500 500 500 500 500 500	NIL
DG Size Q (kVAR)	NIL	242.16 242.16 242.16 242.16 242.16 242.16	NIL
Voltage minimum	0.9119	0.9845	0.9473
Voltage minimum @bus	65	65	NIL
Percentage of loss reduction	NIL	90.220	NIL
Time (sec)	0.5396	3.219	2285.25

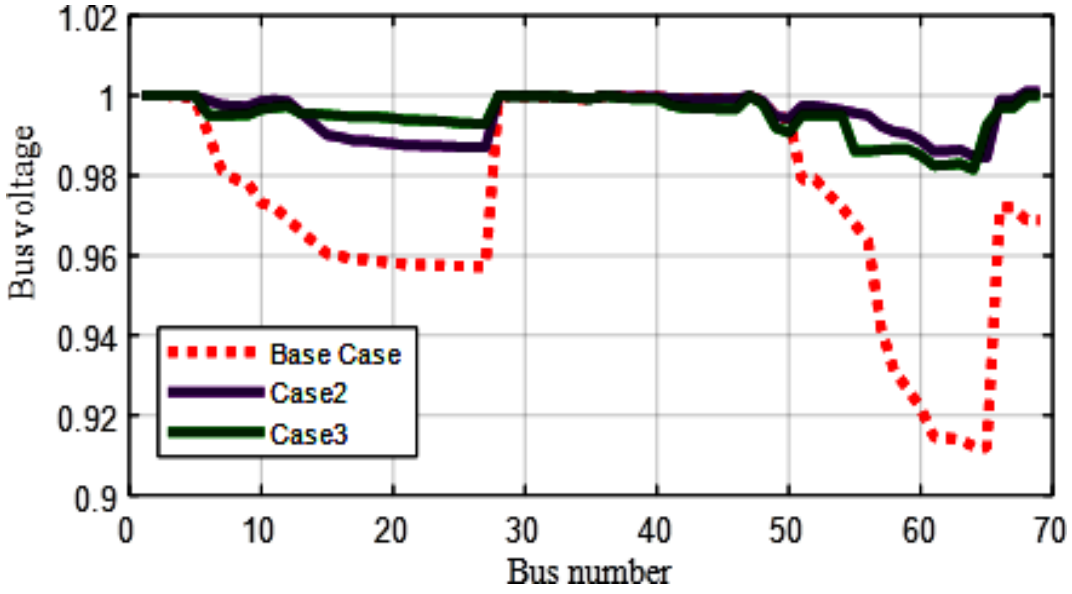

Fig. 8. Voltage profile for CPLM

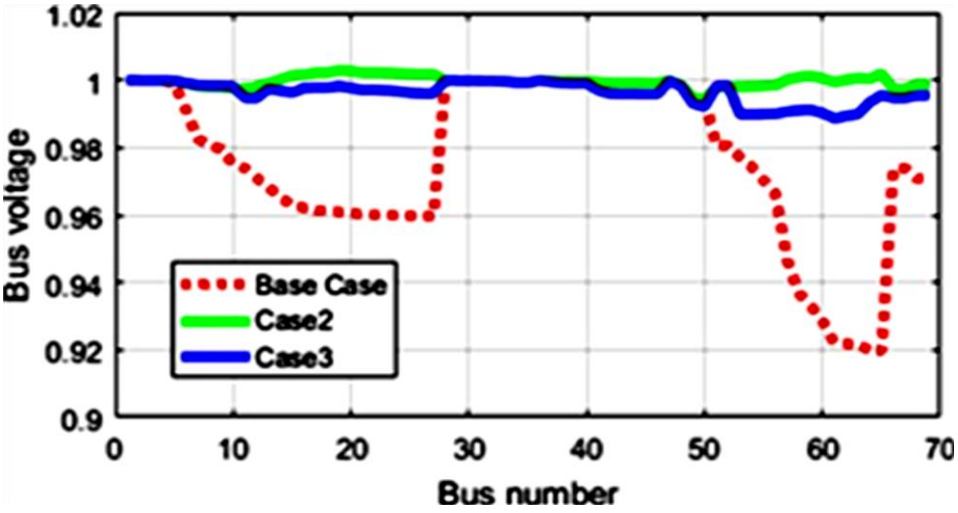

Fig. 9. Voltage profile for CILM

4.6 CILM Analysis for the Modified 69-bus RDS

Table 8 compares the results for the CILM in both cases. The analysis reveals that line loss decreases from 180.67 kW to 11.340 kW in Case 2, and further reduces to 10.960 kW in Case 3. This reduction in real power loss is achieved by installing six DGs units at the following bus locations and capacities: bus 59 (500 kW), bus 62 (500 kW), bus 63 (500 kW), bus 65 (226 kW), bus 69 (173 kW), and bus 19 (500 kW). Fig. 9 illustrates that the voltage deviation in Case 3 follows the trend observed in Case 2. The execution time for Case 2 is 3.2498 seconds, while for Case 3, it is 2078.8749 seconds.

4.7 CZLM Analysis for the Modified 69-bus RDS

Table 9 compares the results for the CZLM in both cases. The analysis shows that line loss decreases from 152.87 kW to 8.885 kW in Case 2, and further reduces to 12.322 kW in Case 3. This reduction in real power loss is achieved by installing six DGs units at the following bus locations and capacities: bus 50 (500 kW), bus 59 (499 kW), bus 64 (500 kW), bus 69 (500 kW), bus 61 (500 kW), and bus 22 (210 kW). Fig. 10 illustrates that the voltage deviation in Case 3 is lower than that in Case 2, indicating that reconfiguration is unnecessary after DG placement. Time taken to execute the result for base_case, case2 and case3 is 0.49343 sec, 3.1866 sec and 2298.8618 sec respectively that shows the execution time increasing from base_case to case 3.

Table 8. Results analysis for case2 and case3 for CILM (modified 69-bus system)

PARAMETERS	BASE_CASE	Case2	Case3
TPL	180.669	11.345	10.969
TQL	83.04	59.694	12.668
Tie Swicth Number	69 70 71 72 73	69 70 71 72 73	52 12 63 15 10
DG Location	NIL	59 62 63 65 69 19	NIL
DG Size P (kW)	NIL	500 500 500 226 173 500	NIL
DG Size Q (kVAR)	NIL	242.16 242.16 242.16 109.45 83.787 242.161	NIL
Voltage minimum	0.9196	0.9942	0.9886
Voltage minimum @bus	65	50	NIL
Percentage of loss Reduction	NIL	93.7203	NIL
Time (sec)	3.249	207	8.874

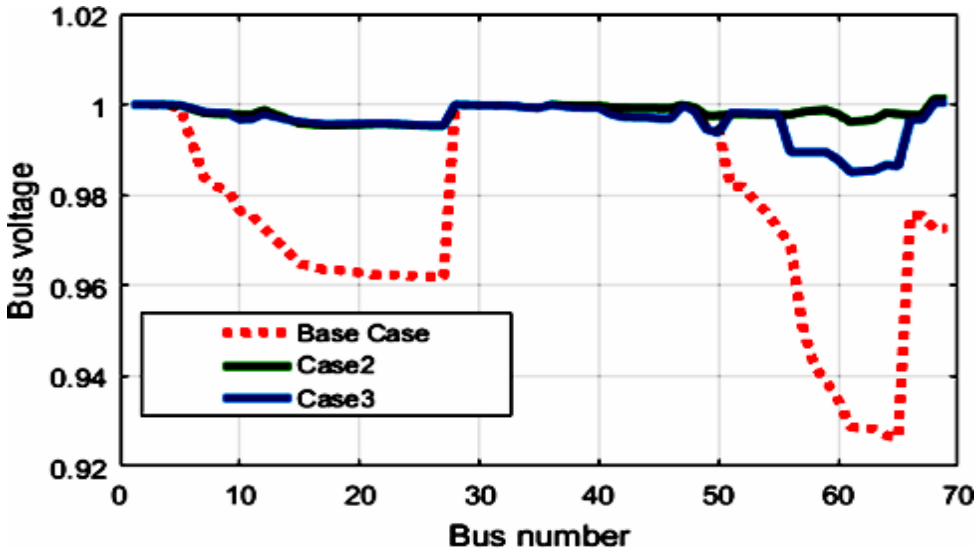

Fig. 10. Voltage deviations for CZLM

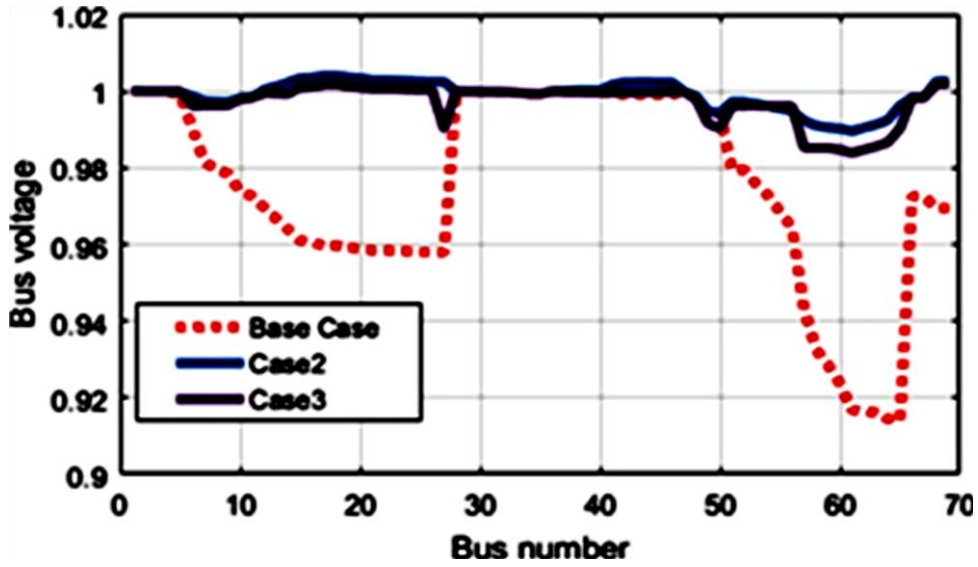

Fig. 11. Voltage deviation for ZIPLM

4.8 ZIPLM Analysis for the Modified 69-bus RDS

Table 10 presents the results for the ZIP load model in both cases. The analysis reveals that line loss decreases from 204.078 kW to 18.1847 kW in Case 2, and further reduces to 16.732 kW in Case 3. This reduction in real power loss is achieved by installing six DGs units at the following bus locations and capacities: bus 62 (468 kW), bus 63 (500 kW), bus 65 (500 kW), bus 69 (448 kW), bus 44 (243 kW), and bus 18 (496 kW). Fig. 11 illustrates that the voltage deviation in Case 3 is improved compared to Case 2. The execution time for Case 2 is 3.2975 seconds, while for Case 3, it is 2321.9955 seconds.

Table 9. Results analysis for case2 and case3 for CZLM (modified 69-bus system)

PARAMETERS	BASE_CASE	Case2	Case3
TPL	152.87	28.8585	12.3225
QPL	71.095	84.659	89.9146
Tie Switch Number	69 70 71 72 73	69 70 71 72 73	55 9 70 73 69
Optimal DG Location	NIL	50 59 64 69 61 22	NIL
Optimal DG Size P (kW)	NIL	500 499 500 500 500 210	NIL
Optimal DG Size Q (kVAR)	NIL	242.16 241.67 242.16 242.16 242.16 101.71	NIL
Voltage minimum	0.9265	0.9952	0.9851
Voltage minimum @bus	65	27	NIL
Percentage of loss Reduction	NIL	94.205	NIL
Time (sec)	0.493	3.187	2298.861

Table 10. Results analysis for case2 and case3 for ZIPLM (modified 69-bus system)

PARAMETERS	BASE_CASE	Case2	Case3
TPL	204.08	18.184	16.732
TQL	93.085	13.039	18.956
Tie Switch Number	69 70 71 72 73	69 70 71 72 73	56 5 26 14 70
DG Location	NIL	62 63 65 69 44 18	NIL
DG Size P (kW)	NIL	468 500 500 448 243 496	NIL
DG Size Q (kVAR)	NIL	226.66 242.16 242.16 216.97 117.69 240.22	NIL
Voltage minimum	0.9141	0.9895	0.9838
Voltage minimum @bus	65	61	NIL
Percentage of loss Reduction'	NIL	91.089	NIL
Time (sec)	0.5208	3.297	2321.995

5 Comparison of the proposed methodology with existing methodologies

To compare the performance of the proposed technique with existing techniques, PSO and GA are applied to the modified 33-bus RDS using the CPLM for Cases 2 and 3. The results of this comparison are presented in Table 11, and the graphical representation is shown in Fig. 14. In PSO_Case 2, The decrease in active power dissipation and reactive power requirements are 47.990 kW and 41.23 kVAR, respectively, achieved by placing two DGs at bus 25 (822 kW) and bus 7 (1000 kW). In GA_Case 2, the savings are 47.0975 kW for real power and 36.0481 kVAR for reactive power, which result from the placement of two DGs at buses 33 (72 kW) and 10 (722 kW). For MWOA_Case 2 with the CPLM, real and reactive power loss savings of 121.3258 kW and 81.7193 kVAR are achieved, with DGs placed at buses 33 (500 kW and 242.161 kVAR), and at bus 15 (500 kW and 242.161 kVAR). Using the CILM in MWOA_Case 2, savings of 127.726 kW in active power and 86.426 kVAR in reactive power, placing DGs strategically at buses 16 (456 kW and 220.851 kVAR), and at buses 31 (434 kW and 210.196 kVAR).

Table 11. Comparison of proposed methodology with existing methodologies (modified 33-bus system)

PARAMETERS	Total Active Power Loss	Total Reactive Power Loss	Tie Switch Number	DG SIZE		DG Type	Voltage Minimum'	Real Power Saving (kW)	Reactive Power Saving (kVAR)
				Active (kW)	Reactive (kVAR)				
BASE_CASE	198.7913	132.682	33 34 35 36 37				0.91377		
PSO_Case2 CPLM	150.875	91.45	33 34 35 36 37	25@822 7@1000		I	.96	47.99	41.232
PSO_Case3 CPLM	120.658	80.56	33 34 35 36 37				.94	78.13	52.232
GA_Case1 CPLM	141.7841	107.8827	10 7 34 32 28				0.93867	57.7913	24.7993
GA_Case2 CPLM	151.6938	96.6339	33 34 35 36 37	33@72 10@722		I	0.95	47.0975	36.0481
GA_Case3_ CPLM	114.3116	72.6087	33 34 35 36 37				0.95	84.4797	60.0733
MWOA_Case2 CPLM	77.4655	50.9627	33 34 35 36 37	33@500 15@500	33@242.16 15@242.16	I,II	0.95615	121.3258	81.7193
MWOA_Case3 CPLM	62.9363	45.2122	7 37 9 13 34				0.96793	135.855	87.4698
MWOA_Case2 CILM	71.0652	46.2557	33 34 35 36 37	16@456 31@434	16@220.85 31@210.20	I,II	0.95721	127.7261	86.4263
MWOA_Case3 CILM	66.8939	49.233	7 37 9 14 34				0.96719	131.8974	83.449
MWOA_Case2 CZLM	65.945	43.7957	33 34 35 36 37	17@463 33@375	17@224.24 33@181.62	I,II	0.95957	132.8463	88.8863
MWOA_Case3 CZLM	71.1006	52.6314	10 28 34 7 14				0.96412	127.6907	80.0506
MWOA_Case2 ZIPLM	78.4176	52.2683	33 34 35 36 37	33@500 18@460	33@242.16 18@222.78	I,II	0.95673	120.3737	80.4137
MWOA_Case3 ZIPLM	63.2221	47.1798	7 37 10 14 34				0.96871	135.5692	84.8202

The active and reactive power loss reductions of 132.84 kW and 88.88 kVAR, respectively, are achieved in MWOA_Case 2 with the CZLM. This is accomplished by placing two DGs at buses 17 (463 kW and 224.2411 kVAR) and 33 (375 kW and 181.6208 kVAR). For the ZIPLM in MWOA_Case 2, the savings in real power loss increase to 120.374 kW, while reactive power savings rise to 80.414 kVAR. These savings are realized by placing two DGs at buses 33 (500 kW and 242.160 kVAR) and 18 (460 kW and 222.780 kVAR). Fig. 12 illustrates the voltage profile for Case 2 across different load models. The performance evaluation of the proposed technique compared to existing techniques (PSO_Case 3 and GA_Case 3) for the CPLM on the modified 33-bus RDS is summarized

in Table 11.

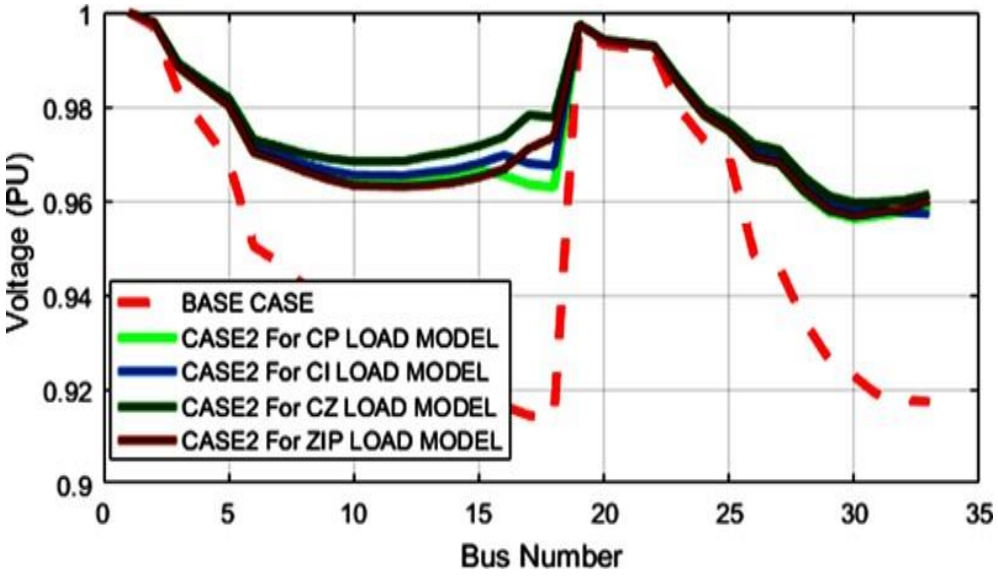

Fig. 12. Voltage profile of case 2 for different load model

The results show that in PSO_Case 3, the real power loss is reduced by 78.13 kW and the reactive power by 52.232 kVAR. In GA_Case 3, the reductions are 84.4797 kW for real power loss and 60.0733 kVAR for reactive power. Using WOA_Case 3 for the CPLM, the savings increase to 121.3258 kW for real power loss and 135.855 kW. with savings in reactive power rising from 81.7193 kVAR to 87.4698 kVAR. For MWOA_Case 3 with the CILM, the active power loss savings increase from 127.726 kW to 131.897 kW, while the reactive power savings decrease slightly from 86.426 kVAR to 83.45 kVAR. In MWOA_Case 3 for the CZLM, real power loss decreases from 132.8463 kW to 127.6907 kW, with reactive power savings reduced from 88.8863 kVAR to 80.0506 kVAR. Finally, with the ZIPLM in MWOA_Case 3, the active power loss savings increase from 120.374 kW to 135.569 kW, while the reactive power savings improve from 80.414 kVAR to 84.820 kVAR. Fig. 13 displays the voltage profile for Case 3 across the various load models.

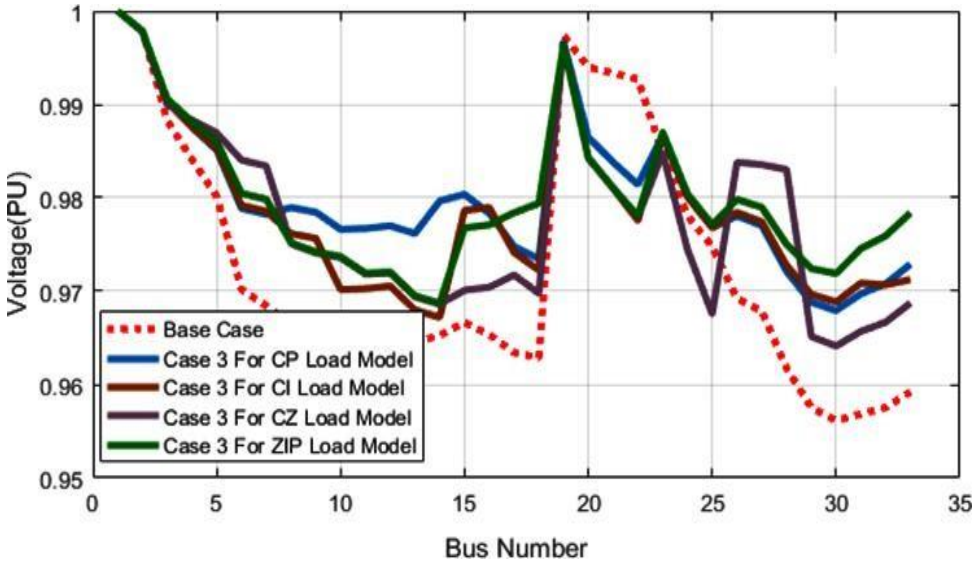

Fig. 13. Voltage deviation of case3 for different load model

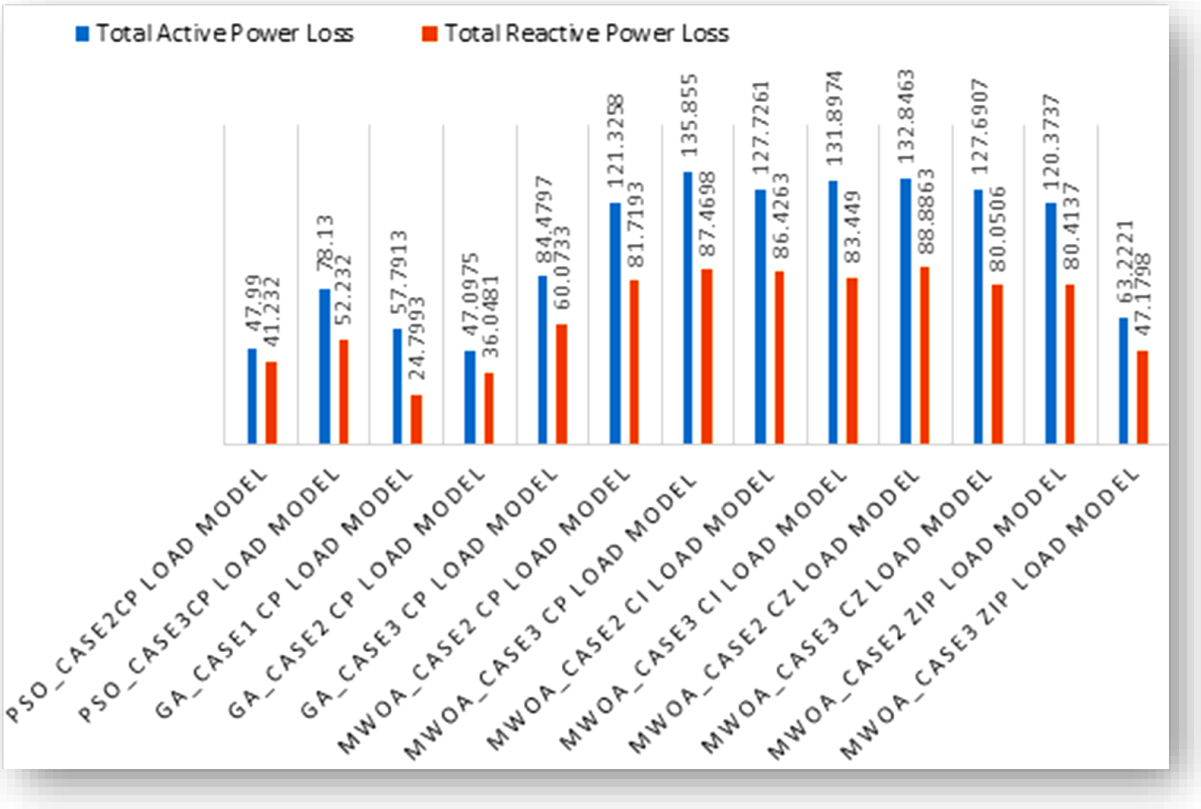

Fig. 14. Comparison of proposed methodology with existing methodologies in terms of active power saving (kW) and reactive power saving (kVAR) for modified 33 bus system

6 Conclusions

In this paper, a methodology for NR after DG placement has been proposed for CP, CI, and CZ load models, along with a ZIP load model considering load variation. The analysis demonstrates that reconfiguration post-DG placement significantly enhances voltage profiles, reduces line losses, and leads to power savings. The findings show that, for the CP and CI load models, the voltage deviation and performance improve after reconfiguration. However, for the CZ load model, reconfiguration after DG placement does not provide additional benefits, indicating that it may not be necessary. The ZIP load model analysis also confirms that the voltage profiles and power savings improve with reconfiguration. Overall, this methodology proves to be an efficient strategy for optimizing power distribution systems, except for the CZ load model, where reconfiguration is not required after DG placement.

References:

[1]. O. Kahouli, H. Alsaif, Y. Bouteraa, N. Ben Ali, and M. Chaabene, "Power System Reconfiguration in Distribution Network for Improving Reliability Using Genetic Algorithm and Particle Swarm Optimization," *Appl. Sci.*, vol. 11, no. 7, pp. 3092, 2021. DOI: https://doi.org/10.3390/app11073092.

[2]. T. Thanh Nguyen, T. Long Duong, and T. Quyen Ngo, "Network Reconfiguration and Distributed Generation Placement for Multi-Goal Function Based on Improved Moth Swarm Algorithm," *Mathematical Problems in Engineering*, vol. 2022, Article ID 5015771, 16 pages, 2022. DOI: https://doi.org/10.1155/2022/5015771.

[3]. P. Dinakara Prasad Reddy, V. C. Veera Reddy, and T. Gowri Manohar, "Whale Optimization Algorithm for Optimal Sizing of Renewable Resources for Loss Reduction in Distribution Systems," *Renewables: Wind, Water, and Solar*, 2017. DOI: 10.1186/s40807-017-0040-1.

[4]. A. Gupta and A. Kumar, "Energy Saving Using D-STATCOM Placement in Radial Distribution System Under Reconfigured Network," *Energy Procedia*, vol. 90, pp. 124-136, Dec. 2016. DOI: https://doi.org/10.1016/j.egypro.2016.11.177.

[5]. K. Sambaiah and T. Jayabarathi, "Optimal Reconfiguration and Renewable Distributed Generation Allocation in Electric Distribution Systems," *International Journal of Ambient Energy*, 2019. DOI: https://doi.org/10.1080/01430750.2019.1583604.

[6]. A. Shaheen, A. Elsayed, A. Ginidi, Ragab El-Sehiemy, and Ehab Elattar, "Reconfiguration of Electrical Distribution Network-Based DG and Capacitors Allocations Using Artificial Ecosystem Optimizer: Practical Case Study," *Alexandria Engineering Journal*, vol. 61, pp. 6105–6118, 2022. DOI: https://doi.org/10.1016/j.aej.2021.11.035.

[7]. T. Thanh Nguyen, T. Long Duong, and T.Quyen Ngo, "Network Reconfiguration and Distributed Generation Placement for Multi-Goal Function Based on Improved Moth Swarm Algorithm," *Mathematical Problems in Engineering*, vol. 2022, Article ID 5015771, 16 pages, 2022. DOI: https://doi.org/10.1155/2022/5015771.

[8]. D. Acheampong, G. Izat Rashed, A. Mensah Akwasi, and H. Haider, "Application of Optimal Network Reconfiguration for Loss Minimization and Voltage Profile Enhancement of Distribution System Using Heap-Based Optimizer," *International Transactions on Electrical Energy Sys- tems*, vol. 2023, Article ID 9930954, 17 pages, Apr. 2023. DOI: https://doi.org/10.1155/2023/9930954.

[9]. S. A. ChithraDevi, L. Lakshminarasimman, and R. Balamurugan, "Krill Herd Algorithm for Multiple DG Placement and Sizing in a Radial Distribution System," *Engineering Science and Technology, an International Journal*, vol. 20, no. 2, pp. 748–759, Apr. 2017. DOI: 10.1016/j.jestch.2016.11.009.

[10]. E. Mahdavi, S. Asadpour, Leonardo, H. Macedo, and R. Romero, "Reconfiguration of Distribution Networks with Simultaneous Allocation of Distributed Generation Using the Whale Optimization Algorithm," *Energies*, vol. 16, no. 12, p. 4560, Jun. 2023. DOI: https://doi.org/10.3390/en16124560.

[11]. M. Esmaeili, M. Sedighizadeh, and M. Esmaili, "Multi-Objective Optimal Reconfiguration and DG (Distributed Generation) Power Allocation in Distribution Networks Using Big Bang-Big Crunch Algorithm Considering Load Uncertainty," *Energy*, vol. 103, pp. 86–99, May 2016. DOI: 10.1016/j.energy.2016.02.152.

[12]. R. Sanjay, T. Jayabarathi, T. Raghunathan, V. Ramesh, and N. Mithulananthan, "Optimal Allocation of Distributed Generation Using Hybrid Grey Wolf Optimizer," *IEEE Access*, vol. 5, pp. 14807–14818, 2017. DOI: 10.1109/ACCESS.2017.2726586.

[13]. I. Hamida, S. Salah, F. Msahli, and M. Mimouni, "Optimal Network Reconfiguration and Renewable DG Integration Considering Time Sequence Variation in Load and DGs," *Renewable Energy*, Jun. 2018. DOI: 10.1016/j.renene.2017.12.106.

[14]. M. Ramesh Babul, C. Venkatesh Kumar, and S. Anitha, "Simultaneous Reconfiguration and Optimal Capacitor Placement Using Adaptive Whale Optimization Algorithm for Radial Distribution System," *Journal of Electrical Engineering & Technology*, Oct. 2020. DOI: https://doi.org/10.1007/s42835-020-00593-5.

[15]. K. Iyer, S. Perumalla, M. Reddy, K. Narayanan, N. Prabaharan, G. Sharma, and T. Senjyu, "Loss Minimization of Distribution Systems by Coordinated Operation of Battery and EVs in the Presence of DGs," *International Transactions on Electrical Energy Systems*, vol. 2023, Article ID 3559846, 12 pages, Apr. 2023. DOI: https://doi.org/10.1155/2023/3559846.

[16]. S. Mirjalili and A. Lewis, "The Whale Optimization Algorithm," *Advances in Engineering Software*, vol. 95, pp. 51–67, May 2016. DOI: https://doi.org/10.1016/j.advengsoft.2016.01.008.

[17]. A.M. Shaheen, A.M. Elsayed, R.A. El-Sehiemy, S. Kamel, S.S.M. Ghoneim, A modified marine predators optimization algorithm for simultaneous network reconfiguration and distributed generator allocation in distribution systems under different loading conditions, *Eng. Optim.* 54 (4) (2022) 687–708, https:// doi.org/10.1080/0305215X.2021.1897799.

[18]. M.-A. Hamidan, F. Borousan, Optimal planning of distributed generation and battery energy storage systems simultaneously in distribution networks for loss reduction and reliability improvement, *J. Energy Storage* 46 (April 2021) (2022) 103844, https://doi.org/10.1016/j.est.2021.103844.

[19].E. Kaushik, V. Prakash, O.P. Mahela, B. Khan, A. El-Shahat, A.Y. Abdelaziz, "Comprehensive overview of power system flexibility during the scenario of high penetration of renewable energy in utility grid", *Energies* 15 (2) (2022), https://doi.org/10.3390/en15020516

[20]. M. Lokesh, M.B. Ravishankar, K.J.S. Kumar, A.D. Kulkarni, "Optimal siting of different levels of DG penetration and its impact on the radial distribution system under different voltage-dependent load models", *Int. J. Renew. Energy Res.* 13 (1) (2023) 474–480, https://doi.org/10.20508/ijrer.v13i1.13701.g8705.

[21].S. Adegoke , Y. Sun, A. Adegoke , D. Ojeniyi "Optimal placement of distributed generation to minimize power loss and improve voltage stability" *Heliyon* 10 (2024) e39298, https://doi.org/10.1016/j.heliyon.2024.e39298.

[22]. A. Chakraborty, S. Ray, "Optimal allocation of distribution generation sources with sustainable

energy management in radial distribution networks using metaheuristic algorithm", *Comput. Electr. Eng.* 116, 109142, February, 2024, https://doi.org/10.1016/j.compeleceng.2024.109142.

[23].J. Sahoo , R. Ray , R. Prakash and S. Sivasubramani, "Impacts of Plug-in EVs and decentralized power generation on distribution system operation, e-Prime - Advances in Electrical Engineering, Electronics and Energy, 9(2024),100658, https://doi.org/10.1016/j.prime.2024.10065.